Future Journal of Pharmaceutical Sciences

RESEARCH Open Access

Development, optimization and characterization of flurbiprofen matrix transdermal drug delivery system using Box–Behnken statistical design

Ramakant Joshi* and Navneet Garud

Abstract

Background: Present investigation for research was to develop matrix-type transdermal drug delivery system of flurbiprofen (FBP) with the various ratio of matrix polymers (hydrophilic and hydrophobic), the concentration of plasticizer and natural penetration enhancer by Box–Behnken statistical design to investigate the combined outcome of selected independent variables for effective management of rheumatoid arthritis.
The influence of a binary mixture of polymers, plasticizer and penetration enhancer on physicochemical considerations including thickness, tensile strength, percent elongation, weight variation, percent moisture content, percent moisture uptake, water vapour transmission rate, folding endurance, drug content, in vitro drug dissolution study and then ex vivo drug permeation study was evaluated.

Results: The study demonstrated that the tensile strength of films improved by matrix polymer ratio and to a slighter gradation in the rise of plasticizer and natural penetration enhancer. Ex vivo drug permeation study was accompanied via excised porcine skin as a permeation barrier in Franz diffusion cell. Ex vivo drug permeation study indicated that matrix polymer ratio (HPMC K15M:ERL100) at 3:1 and natural penetration enhancer (d-limonene) at highest concentration 7.5% w/w containing formulation FBPT7 delivered maximum flux and supplementary improved the permeation of drug. The result of the skin irritation test revealed that the developed formulation is free from any type of skin irritation effects like erythema and oedema.

Conclusion: Based on the findings of this research, it can be established that a well-controlled release and very effective skin penetration of the drug was accomplished by the film FBPT7 in the existence of permeation enhancers for prolonged periods.

Keywords: Transdermal drug delivery system, Box–Behnken statistical design, Rheumatoid arthritis, Flurbiprofen, Natural penetration enhancer

Background

The goal line of the recent therapeutic investigation is to discover a drug candidate through necessary therapeutic action and fewer side effects. Discovering the new drug molecules is very costly; therefore, another method of improving therapeutic efficacy is the development of a new drug delivery system that achieves pharmaceutical selectivity not only based on the chemical structure but also the basis of pharmacokinetic principle. So scientists are centring on the research and advance of novel drug delivery system which is proficient in monitoring the rate of drug delivery, sustaining the extent of therapeutic action and targeting the delivery of the drug to the infected tissue or organ. To grow the value, there are various

* Correspondence: Joshiram78@gmail.com
School of Studies in Pharmaceutical Sciences, Jiwaji University, Gwalior (M.P)-474011, India

Springer Open

© The Author(s). 2021 **Open Access** This article is licensed under a Creative Commons Attribution 4.0 International License, which permits use, sharing, adaptation, distribution and reproduction in any medium or format, as long as you give appropriate credit to the original author(s) and the source, provide a link to the Creative Commons licence, and indicate if changes were made. The images or other third party material in this article are included in the article's Creative Commons licence, unless indicated otherwise in a credit line to the material. If material is not included in the article's Creative Commons licence and your intended use is not permitted by statutory regulation or exceeds the permitted use, you will need to obtain permission directly from the copyright holder. To view a copy of this licence, visit http://creativecommons.org/licenses/by/4.0/.

limitations of the oral conventional drug delivery system like tablets, capsules, etc. This is more dangerous to drugs whose toxic and therapeutic drug levels are close or have a narrow therapeutic range. So by developing the controlled release drug delivery system, a constant or zero-order drug release will be achieved [1, 2].

The challenge posed by the stratum corneum that hampers drug permeation is the issue associated with the transdermal route of drug administration. Concerning the form of the molecule, it requires to be carried through the skin, and this layer is very selective; therefore, only molecules with unique physicochemical properties can sufficiently travel through the skin [3]. This leads to the variety of available transdermal drugs that can be delivered to be very limited, which demonstrates the need to integrate penetration enhancers into formulations that could help distribute a broader range of drugs efficiently [4]. Via one or more of the mechanisms interacting with stratum corneum (SC) lipids and/or keratin, terpenes can increase skin permeation and increase drug solubility into SC lipids [5]. On the other hand, the potential of terpenes as percutaneous absorption enhancer was suggested [6]. Several cyclic terpenes like cineole, d-limonene and α-pinene have been intensively investigated as penetration enhancers.

Rheumatoid arthritis (RA) is an inflammatory condition characterized by chronic inflammation of the joints, prominent eventually to serious injury and premature mortality [7]. RA causes prolonged synovial membrane inflammation and this leads to periarticular bone degradation, deterioration of articular cartilage and permanent deformities, along with signs of extra-articular disease as the disease progresses [8]. Owing to their analgesic as well as anti-inflammatory actions, nonsteroidal anti-inflammatory medications (NSAIDs) are the most frequently and generally used drugs for the treatment of arthritis disorders. These function by inhibiting the enzyme cyclooxygenase (COX) involved in the transformation of arachidonic acid into prostaglandins [9]. Flurbiprofen (FBP), a derivative of phenyl propionic acid, has demonstrated analgesic, anti-inflammatory and antipyretic capabilities for the treatment of pain in RA in humans. Like other NSAIDs, the anti-inflammatory action of flurbiprofen has been linked to the reversible inhibition of COX, which is responsible for the transformation of arachidonic acid to prostaglandin G2 (PGG2) and PGG2 to prostaglandin H2 (PGH2) in the prostaglandin synthesis path. The concentration of prostaglandins responsible for inflammation, pain, swelling and fever is effectively decreased by this alteration. Low aqueous solubility and certain severe abdominal side effects, such as GI irritation, GI bleeding etc., grasp back the RA therapy applications of this wonderful NSAID member. FBP has shown that its great lipophilicity explains its low bioavailability afterwards oral route administration and short half-life 3.9 h due to which frequent dosing is required [10, 11]. These shortcomings can be conquered by the advancement of the transdermal drug delivery system.

Methods

Materials

Flurbiprofen (FBP) was acquired from FDC Ltd. Dist. Roha Dist. Raigarh, Maharashtra, as a gift sample. Eudragit RL 100 (ERL100) was procured as a gift sample from Evonik India Pvt. Ltd., Mumbai, Maharashtra. Hydroxy propyl methyl cellulose (HPMC K15M) was procured as a gift sample from Colorcon Asia Pvt. Ltd (India), Goa. D-limonene was received as a gift sample from Shakti Enterprise Mumbai, Maharashtra. Di-butyl phthalate was bought from Loba Chemie, Mumbai, Maharashtra. Altogether additional chemicals and solvents were of analytical reagent grade.

Animals

Twelve Albino Wistar male rats (6–8 weeks old), weighing 180–220 g, were taken for the experiment. We collected rats from M/S Chakraborty Enterprise, Kolkata. The animals were kept in typical controlled environments at temperature 22 ± 1 °C to 30 ± 1 °C, relative humidity 35 ± 5 to 65 ± 5%, and kept underneath 12/12-h light/dark cycles with free access to food and water ad libitum. At the end of the observation period, all rats were euthanized using an overdose of ketamine (i.p) anaesthesia. All sections of this report adhere to the Animal Research: Reporting of In Vivo Experiments guidelines for reporting animal research.

The study protocol was approved by the Institutional Animal Ethical Committee (IAEC) according to the protocols permitted by the Committee for Purpose of Control and Supervision of Experiments on Animals (CPCS EA), Ministry of Social Justice and Empowerment, Government of India, under the reference no. IAEC/JU/50 on the recommendations of the Institutional Animal Ethical Committee.

Statistical investigational design

To optimize the formulation factors and formulation variables, a three-factor, three-level Box–Behnken statistical architecture was used for the evaluation of transdermal film of FBP (Design-Expert 11.1.0.1 Stat Ease Inc., Minneapolis, MN, USA) [12]. Based upon the initial trial study, three independent variables used in the experimental design namely polymer (HPMC K15:ERL100) ratio as film-forming polymers, the concentration of dibutyl phthalate (% w/w) as plasticizer and the concentration of d-limonene (% w/w) as penetration enhancer

with dependent variables namely tensile strength (kg/cm^2), steady-state flux (μg/cm^2/h) and the cumulative amount of drug permeated in 24 h (Q_{24}) (μg/cm^2) were a selection of current approach [13]. The coding and definite values of independent variables are listed down in Table 1.

The polynomial equation was produced accordingly:

$$R = \beta 0 + \beta 1A + \beta 2B + \beta 3C + \beta 4AB + \beta 5AC + \beta 6BC + \beta 7A^2 + \beta 8B^2 + \beta 9C^2$$

Here *R* represents response, whereas *A*, *B* and *C* denote the independent variables, i.e. polymer (HPMC K15:ERL100) ratio, the concentration of plasticizer and the concentration of penetration enhancer, respectively. The *β*0 value signifies the resultant regression coefficient. The experimentation was randomized to exploit the consequence of unexplained variability on perceived reactions owing to exogenous factors. *AB*, *AC* and *BC* rise by communication of independent variables, explains the deviations in response to changes within these factors.

Formulation of matrix-type transdermal film

The matrix type of the transdermal film was formulated by the solvent evaporation method by pouring the polymeric solution in the mercury-containing Petri plate. The different composition of the matrix-forming polymer ratio of HPMC K15M and ERL100 (Table 2) was dissolved in dicholormethane: methanol (1:1) solvent system and allowed to swell for 2 h. The separately formed drug solution (15.8% w/w based on total polymer weight) in ethanol was mixed homogeneously to matrix polymeric solution with constant stirring. A known quantity of di-butyl phthalate (DBT) as a plasticizer was added to the solution. Prefix quantity of d-limonene as a penetration enhancer was added dropwise to the polymeric solution. The resultant drug–polymer matrix solution was discharged into a Petri plate using a fabricated glass ring of 10 cm^2. An inverted funnel was positioned for covering the Petri plate for controlling the rate of solvent evaporation and maintained for 48 h at room temperature to get the dried film. Afterwards, complete drying the film was cut down in 3.14 cm^2 size for further evaluation and retained in a desiccator comprising silica as a desiccant for further analysis [14].

Fourier transform infrared spectroscopy (FT-IR) study

To investigate the possible chemical interfaces between drug (FBP) and polymers (HPMC K15M and ERL100), a spectral research review of FT-IR was conducted on the FT-IR spectrophotometer (Perkin Elmer Model No. Spectrum Two Serial no. 105627 FT-IR). Different samples were combined with KBr and crushed to yield pellets at a pressure of 150 kg/cm^2. In the 4000–400-cm^{-1} area, FT-IR spectra from pure FBP, HPMC K15M, ERL100 and their physical mixture were scanned [15].

Differential scanning calorimetry (DSC) study

For FBP, HPMC K15M, ERL100 and their physical mixture differential scanning calorimetry (DSC) measurements were carried out using a DSC instrument (Shimadzu Model No. DSC-60Plus) furnished with a liquid nitrogen sub-ambient accessory. The instrument worked at a rate of 20 ml/min under a nitrogen purge gas. Samples (3–6 mg) were weighed in open aluminium pans and screened from 30–300 °C at a speed of 10 °C/min [16].

Physicochemical characterization of the transdermal film

Film thickness

Film thickness via a digital Vernier calliper was measured at six different places (Stanley, New Delhi, India) by selecting three films randomly from each batch to confirm the constant thickness. The mean and standard deviation values were determined [17].

Tensile strength

Tensile strength gives an idea about the film's mechanical property and strength. It was determined by an instrument pulley system constructed upon laboratory level. The one end of the transdermal film was fixed and another end of the film which was tied with thread was thrown over a freely moving pulley. The weight on the pan gradually enough to breakdown the film was noted down [18]. The tensile strength was considered with the following equation:

Table 1 Independent variables and levels of experimental design

S.No.	Independent variables	Code level		
		Low (− 1)	Mid (0)	High (+ 1)
1.	*A* = polymer (HPMC K15M: ERL100) ratio	1:1	2:1	3:1
2.	*B* = concentration of di-butyl phthalate (% w/w)	20	30	40
3.	*C* = concentration of d-limonene (% w/w)	2.5	05	7.5

Table 2 Test design and results of response surface analysis

Run	Formulation code	Independent Variables			Dependent variables			Permeability coefficient K_p (cm/h)	Enhancement ratio
		A	*B*	*C*	R_1 (kg/cm^2)	R_2 (μg/cm^2/h)	R_3 (μg/cm^2)		
1	FBPT1	3:1	40	5	3.067 ± 0.234	387.99 ± 5.054	7256.7 ± 7.593	$1.293 \times 10^{-2} \pm 0.214$	3.650
2	FBPT2	3:1	20	5	3.317 ± 0.129	378.07 ± 7.102	7166.16 ± 2.494	$1.260 \times 10^{-2} \pm 0.136$	3.557
3	FBPT3	2:1	20	2.5	2.570 ± 0.037	313.16 ± 4.872	5475.3 ± 4.289	$1.043 \times 10^{-2} \pm 0.089$	2.946
4	FBPT4	2:1	40	7.5	2.348 ± 0.021	434.32 ± 9.762	7856.05 ± 6.888	$1.447 \times 10^{-2} \pm 0.307$	4.086
5	FBPT5	1:1	30	2.5	2.216 ± 0.210	296.45 ± 6.412	5286.44 ± 8.539	$0.988 \times 10^{-2} \pm 0.075$	2.789
6	FBPT6	2:1	30	5	1.958 ± 0.110	392.67 ± 3.017	7190.05 ± 5.998	$1.308 \times 10^{-2} \pm 0.432$	3.694
7	FBPT7	3:1	30	7.5	2.783 ± 0.312	468.97 ± 8.294	8543.17 ± 1.939	$1.563 \times 10^{-2} \pm 0.065$	4.412
8	FBPT8	1:1	40	5	2.489 ± 0.109	351.95 ± 2.829	6485.15 ± 3.228	$1.173 \times 10^{-2} \pm 0.245$	3.311
9	FBPT9	1:1	20	5	2.230 ± 0.299	336.73 ± 4.210	6165.20 ± 9.298	$1.112 \times 10^{-2} \pm 0.121$	3.168
10	FBPT10	1:1	30	7.5	2.279 ± 0.023	380.73 ± 10.989	6943.41 ± 4.328	$1.269 \times 10^{-2} \pm 0.092$	3.582
11	FBPT11	2:1	20	7.5	2.016 ± 0.205	423.91 ± 7.503	7797.18 ± 3.293	$1.413 \times 10^{-2} \pm 0.342$	3.988
12	FBPT12	2:1	30	5	2.184 ± 0.319	394.11 ± 3.456	6931.19 ± 6.674	$1.313 \times 10^{-2} \pm 0.043$	3.708
13	FBPT13	2:1	30	5	2.078 ± 0.461	401.63 ± 11.229	6535.14 ± 2.738	$1.338 \times 10^{-2} \pm 0.099$	3.778
14	FBPT14	2:1	30	5	2.117 ± 0.120	388.67 ± 6.820	6912.86 ± 7.547	$1.295 \times 10^{-2} \pm 0.032$	3.657
15	FBPT15	3:1	30	2.5	3.128 ± 0.009	326.46 ± 12.482	6085.77 ± 6.837	$1.088 \times 10^{-2} \pm 0.164$	3.071
16	FBPT16	2:1	40	2.5	2.036 ± 0.223	318.78 ± 8.421	5579.17 ± 10.378	$1.062 \times 10^{-2} \pm 0.204$	2.999
17	FBPT17	2:1	30	5	2.117 ± 0.199	376.93 ± 5.999	6793.44 ± 5.253	$1.256 \times 10^{-2} \pm 0.254$	3.546

Values are expressed as mean ± S.D., $n = 3$

$$\text{Tensile Strength} = \frac{F}{a.b\left(1+\frac{L}{E}\right)} \quad (1)$$

where

a = width of the film, b = thickness of the film, F = break force, L = length of the film and E = elongation of the film

The percent elongation was measured by length just before the breakpoint which is called the length of the film after elongation (L_2) subtracting the initial length of the film (L_1) divided by the initial length of the film [19].

$$\%\text{Elongation} = \left[\frac{L2-L1}{L1}\right]100 \quad (2)$$

wherever

L_1 = initial length of the film and L_2 = length of the film after elongation

Weight variation

The transdermal film weight was estimated by randomly choosing 10 films from each batch that were independently weighted and then the mean weight was measured. The difference in weight was calculated by the distinction between mean weight and individual weight.

% Moisture content

The moisture content in the transdermal film was determined by individually weighing and placing in an anhydrous calcium chloride-containing desiccator at room temperature (25 °C) for 24 h. Afterwards, the film was repetitive until a constant weight was attained. The percent moisture content was designed by the difference amongst the final weight of the film and the initial weight of the film divided by initial weight [20].

$$\%\text{Moisture content} = \frac{W2-W1}{W1} \times 100 \quad (3)$$

where

W_2 = final weight of the film and W_1 = initial weight of the film

% Moisture uptake

The moisture uptake was determined by accurately weighing the transdermal film and keeping in a desiccator comprising a saturated solution of potassium chloride at 84% RH and room temperature, and then after 3 days, the film was reweighed. The percent moisture uptake was calculated by the difference between the final weight of the film and the initial weight of the film divided by the initial weight [21].

$$\%\text{Moisture uptake} = \frac{W2-W1}{W1} \times 100 \quad (4)$$

where

W_2 = final weight of the film and W_1 = initial weight of the film

Water vapour transmission rate

Equal-diameter glass vials that were used as transmitting cells were carefully cleaned and dried in the oven. The cells were placed with around 1 g of anhydrous calcium chloride and the respective polymer film was fixed over the brim. The cells were precisely weighted and kept in a closed desiccator containing potassium chloride saturated solution to preserve 84% relative humidity. The cells were separated and measured within 24 h [22]. Using the following formula, the volume of water vapour transmitted was determined:

$$\text{Water vapour transmission rate} = \frac{W2 - W1}{T \times A} \times 100 \quad (5)$$

where

W_2 = final weight of the film, W_1 = initial weight of the film, T = time of exposure and A = area of the film

Folding endurance

The film's folding endurance was measured by constantly folding the film in the same place before it separated. The folding durability value was the number of times the film could be folded in the same position without splitting [23].

Drug content

Films of recognized areas were reserved in 10 ml of the volumetric flask for drug content analysis and casting solvent mixture was applied to it. The flasks were shaken at 37 °C for 24 h in a water bath. The solution was then screened into Whatman filter paper No. 1 and diluted correctly before testing the drug content via a UV–visible spectrophotometer (UV-1800, SHIMADZU, Japan) at 247 nm [24].

In vitro drug dissolution study

Transdermal film dissolution study was accomplished by the USP Dissolution Apparatus V paddle over the disc. The films were put with their drug matrix exposed to the phosphate buffer pH 7.4, in the corresponding baskets. Entire dissolution experiments were conducted at 32 °C, at 50 rpm, with 900 ml of buffer in each dissolution vessel. Samples were obtained at various periods and evaluated in contrast to the blank using a UV spectrophotometer at 247 nm. Cumulative quantities of drug released for various formulations were plotted against time [25].

Model fitting

Kinetic models in which the dissolved quantity of the drug (Q) is a function of the test time, t, or $Q = f_{(t)}$, have defined drug dissolution from solid dosage forms. Any $Q_{(t)}$ function theoretical concepts are widely used, such as models of zero order, first order, Hixson–Crowell, Higuchi and Korsmeyer–Peppas.

Ex vivo drug permeation study

Skin preparation

Excised porcine skin was used for the ex vivo permeation studies. Excised porcine skin was obtained from the local slaughter house after sacrificing the animal within 1 h. The hair was removed from the upper portion of the excised skin surface using an animal hair clipper and, subsequently, the full thickness of the skin was collected. The fatty layer, adhering to the dermis side, was removed by a surgical scalpel. The pieces of skin were washed three times with a pH 7.4 phosphate buffer and wrapped in an aluminium foil. It was then kept for analysis in a deep freeze [26].

Drug permeation study

For the ex vivo permeation experiments, a Franz diffusion cell with a surface area of 3.14 cm^2 was used. Between the compartments of the diffusion cell and the stratum corneum facing the donor compartment, the excised porcine skin was placed. In the procedure, the stratum corneum side of the skin was held in near touch with the transdermal film. The receiver compartment held 15 ml of PBS pH 7.4, stirred at 100 rpm with a magnetic stirrer. The entire assembly was retained on a magnetic stirrer, and at 37 ± 0.5 °C, the analysis was carried out. The quantity of the permeated drug substance was calculated by extracting 1 ml of aliquots from the receptor fluid at predetermined time points up to 24 h and replenishing them with an equivalent quantity of fresh medium. Samples were purified using Whatman filter paper and spectrophotometrically measured the absorbance at 247 nm. The cumulative amount of drug permeated per cm^2 was estimated and plotted over time [21].

Skin irritation test

Based upon the modified Draize test system on healthy Wistar male rats weighing between 180 and 220 g, the skin irritation test was performed. The animals were randomly divided into four classes (n = 3) and the hair was removed 24 h before the test from the dorsal region of the Wistar male rats. Group I was classified as a negative control group, group II was applied as an adhesive tape, group III was obtained as a test formulation and group IV was applied as a positive control group with normal irritant formalin (0.8% v/v). The 3.14-cm^2 area membranes were used as test transdermal films. The

research was performed on unbroken rat skin. The transdermal films were extracted with the help of an alcohol swab after the duration of 48 h. The experimental study was carried out with the application of new films or new formalin solution for 7 days. Erythema/oedema was tested on the skin and the application locations were assessed on a visual rating scale, all by the same investigator [27].

Results

Fourier transform-infrared spectroscopy (FT-IR) study

The FT-IR spectral investigation of FBP gives a characteristic sharp peak at 1701.83 cm^{-1} demonstrating the existence of (C=O) carbonyl compound stretching, a peak at 1128.89 cm^{-1} denoting stretching of (C–F) and a characteristic broad peak of FBP showing O–H stretching of the acidic group at 3369.64 cm^{-1}, approving the pureness of drug (Fig. 1). The FT-IR spectra of the ternary combinations FBP:HPMC K15M:ERL100 exhibited that the chief peaks of FBP were retained and detected at wavenumbers 3369.64, 1696.06 and 1128.25 cm^{-1}. The existence of polymers (hydrophilic and hydrophobic) did not perform to considerably affect the integrity of the FBP peaks.

Differential scanning calorimetry (DSC) study

DSC investigation of FBP, HPMC K15M, ERL100 and their physical mixture is presented in the figure. FBP displayed a sharp endothermic peak at 118.15 °C. The thermal behaviour of HPMC K15M and ERL100 demonstrated no such phenomenon in any temperature intervals. The presence of a peak corresponding to the melting of FBP in the physical mixture thermogram was also evident. In the existence of polymeric materials, the results indicated a negligible change in the melting point of FBP (Fig. 2).

Physicochemical characterization of the transdermal film

The outcomes of the physicochemical characterization of transdermal films are revealed in Table 3. Entirely films have a flat and smooth surface that is suitable for application to the skin. The thickness of the prepared

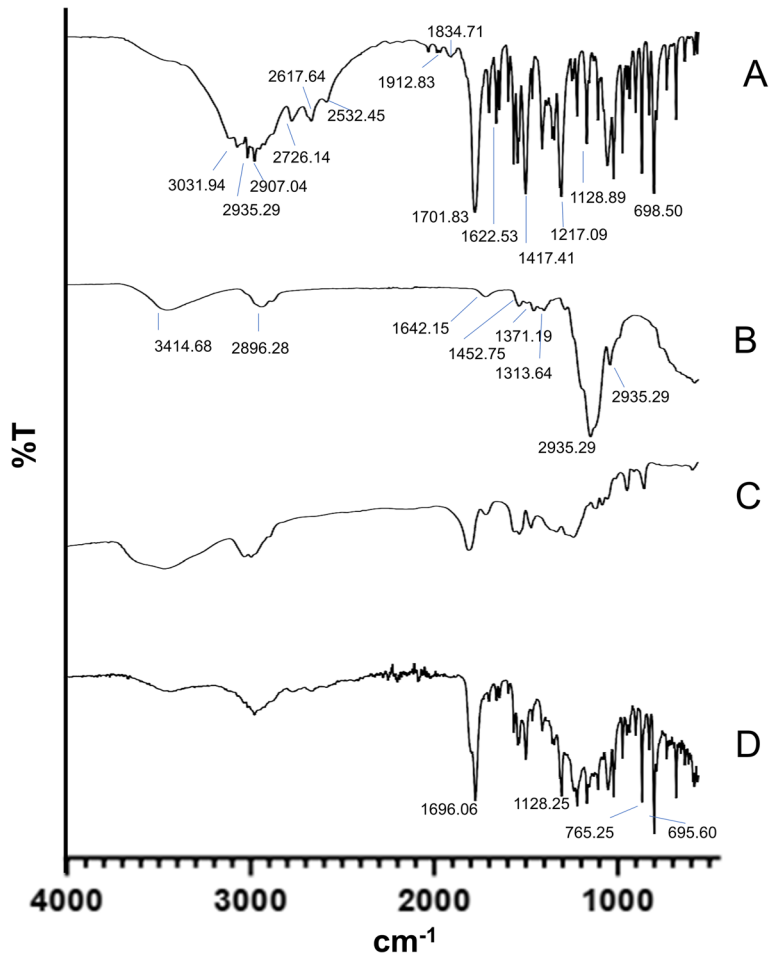

Fig. 1 FT-IR spectra of (**a**) pure flurbiprofen, (**b**) HPMC K15M, (**c**) ERL100 and (**d**) drug and polymer physical mixture

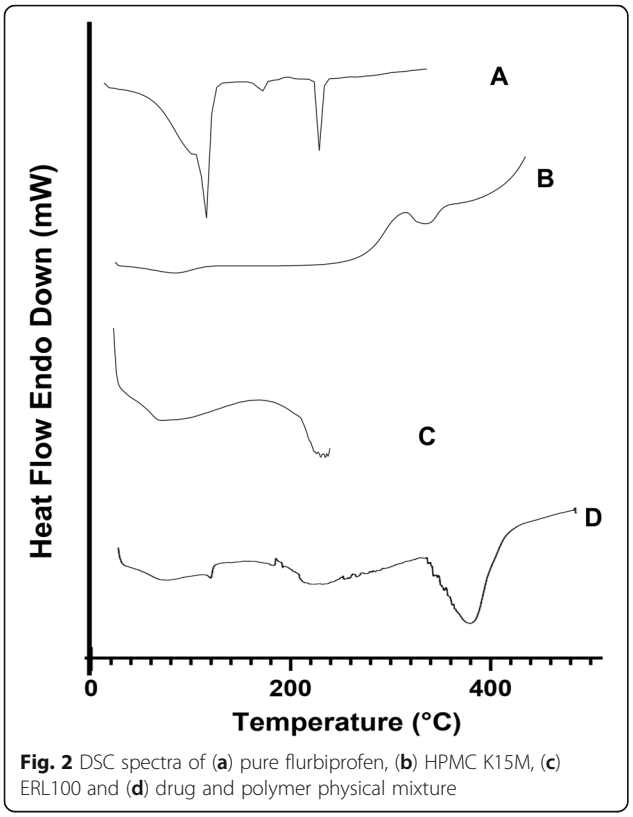

Fig. 2 DSC spectra of (**a**) pure flurbiprofen, (**b**) HPMC K15M, (**c**) ERL100 and (**d**) drug and polymer physical mixture

transdermal film was ranging between 0.483 ± 0.083 and 0.564 ± 0.029 mm. Tensile strength indicates the strength and mechanical property of the film. The results for tensile strength were 1.958 ± 0.110 to 3.317 ± 0.129 kg/cm^2. The weight of films was observed between 117.17 ± 0.173 and 122.46 ± 0.193mg. This revealed that change in the polymer ratio has no noteworthy effect on the weight of the film.

The outcomes for percent moisture content, percent moisture uptake and water vapour transmission rate was ranged between 1.92 ± 0.085 and 5.58 ± 0.118, 5.79 ± 0.110 and 12.67 ± 0.200, 0.67 ± 0.073 and 3.08 ± 0.057 g/cm^2/h, respectively. The findings showed that the rise in hydrophilic polymer concentration was directly proportionate to the upsurge in the film's moisture content and moisture uptake. The water vapour transmission rate was decreased due to an increase in the hydrophobic polymer portion. The results for folding endurance were 112 ± 2.867 to 188 ± 1.248. Folding endurance aims to assess the capability of the film to survive breakup as it is applied to the surface of the skin. The maximum value for folding endurance reflects that film would sustain its integrity and shape through the course of application. Uniformity of drug content was detected amongst all formulation code and ranged between 96.39 ± 0.215 and 99.88 ± 0.049%.

Optimization of the formulation by experimental design

In Tables 1 and 2, the independent variables and responses for all 17 experiments are given. Figures 3, 4 and 5 display the contour plots and 3D response surface plots drawn using Design-Expert tools. Design-Expert software was used to optimize the formulation and progress the quadratic Eqs. 6, 7 and 8.

Tensile strength response

Response 1: Tensile strength

The 53.06 Model F value implies that the model is significant. p values of less than 0.0500 demonstrate that model terms are significant. A, B, A^2 and B^2 are important model words in this case. Values greater than 0.1000 mean the terms of the model are not significant. In contrast to the pure error, the Lack of Fit F value of 0.6468 means that the Lack of Fit is not significant. There is a 62.47% probability due to noise that a loss of Match F value this high will occur. Non-substantial lack of fit is fine.

The test results in Table 4 are equipped with regression, and the final equation for data analysis to achieve the coding factor is seen in Eq. (6).

$$\begin{aligned} \text{R1 (Tensile Strength)} = {} & 2.09 + 0.3851{*}\text{A-}0.0241{*}\text{B-}0.0655 \\ & {*}\text{C-}0.1273{*}\text{AB-}0.1020{*}\text{AC} \\ & +0.2165{*}\text{BC} + 0.5220{*}\text{A}^2 \\ & +0.1630{*}\text{B}^2\text{-}0.0113{*}\text{C}^2 \end{aligned} \tag{6}$$

The overall p value of the model is $0.0001 < 0.05$, showing that the regression function is precisely significant, and the "lack of p value fitting" is $0.6247 > 0.05$, implying that the lack of fitting is insignificant. It means that the equation's fitting degree is comparatively fine. Regression analysis of the experimental regression equation (Table 4) showed that the terms A^2 and B^2 had a very important influence on transdermal film tensile strength. There was an important influence of the plasticizer on tensile strength ($p < 0.05$).

Steady-state flux response

Response 2: Steady-state flux

The 47.54 Model F value means that the model is significant. p values of less than 0.0500 demonstrate that model terms are significant. A and C are important model terms in this case. Values greater than 0.1000 mean the terms of the model are not relevant. In contrast to the pure error, the Lack of Fit F value of 0.8893 means that the Lack of Fit is not significant. There is a 51.92% probability due to noise that a loss of Match F value this high will occur. Non-substantial lack of fit is fine.

Table 3 Physicochemical characterization of flurbiprofen transdermal film

S.No.	Formulation code	Thickness (mm)	Weight (mg)	% Moisture content	% Moisture uptake	Water vapour transmission rate (g/cm^2/h)	Folding endurance (no. of folds)	Drug content (%)
1	FBPT1	0.555 ± 0.007	117.92 ± 0.288	4.57 ± 0.081	10.86 ± 0.250	2.98 ± 0.304	184 ± 2.282	98.72 ± 0.231
2	FBPT2	0.541 ± 0.021	117.49 ± 0.538	5.30 ± 0.126	11.92 ± 0.287	2.72 ± 0.181	164 ± 1.632	99.06 ± 0.193
3	FBPT3	0.505 ± 0.013	119.65 ± 0.340	3.29 ± 0.116	10.13 ± 0.054	1.85 ± 0.094	132 ± 0.669	99.41 ± 0.309
4	FBPT4	0.522 ± 0.032	121.22 ± 0.261	4.06 ± 0.041	9.16 ± 0.391	1.46 ± 0.037	138 ± 0.816	97.32 ± 0.012
5	FBPT5	0.492 ± 0.064	117.44 ± 0.755	2.29 ± 0.156	6.46 ± 0.286	0.79 ± 0.044	121 ± 2.941	98.48 ± 0.470
6	FBPT6	0.514 ± 0.082	120.55 ± 0.253	3.80 ± 0.181	7.84 ± 0.319	2.06 ± 0.066	159 ± 1.414	98.83 ± 0.172
7	FBPT7	0.537 ± 0.022	118.16 ± 0.338	4.95 ± 0.060	11.26 ± 0.246	2.53 ± 0.118	171 ± 3.558	99.18 ± 0.135
8	FBPT8	0.506 ± 0.037	121.82 ± 0.231	1.92 ± 0.085	5.79 ± 0.110	1.07 ± 0.012	112 ± 2.867	96.39 ± 0.215
9	FBPT9	0.493 ± 0.041	119.41 ± 0.340	2.33 ± 0.134	7.28 ± 0.131	1.47 ± 0.838	127 ± 3.091	97.09 ± 0.097
10	FBPT10	0.497 ± 0.083	117.17 ± 0.173	2.82 ± 0.193	6.87 ± 0.015	0.67 ± 0.073	147 ± 3.741	98.37 ± 0.126
11	FBPT11	0.525 ± 0.091	118.35 ± 0.211	4.35 ± 0.215	8.99 ± 0.155	1.96 ± 0.050	160 ± 0.943	98.95 ± 0.290
12	FBPT12	0.536 ± 0.074	120.51 ± 0.298	3.82 ± 0.082	9.30 ± 0.169	1.78 ± 0.092	153 ± 2.160	96.97 ± 0.085
13	FBPT13	0.483 ± 0.083	122.20 ± 0.162	4.16 ± 0.110	9.65 ± 0.167	2.22 ± 0.020	142 ± 0.473	97.67 ± 0.280
14	FBPT14	0.514 ± 0.009	121.80 ± 0.112	4.95 ± 0.115	10.55 ± 0.134	1.58 ± 0.164	145 ± 2.490	98.60 ± 0.103
15	FBPT15	0.564 ± 0.029	117.28 ± 0.826	5.58 ± 0.118	12.67 ± 0.200	3.08 ± 0.057	188 ± 1.248	98.02 ± 0.032
16	FBPT16	0.515 ± 0.048	122.46 ± 0.193	2.70 ± 0.254	10.22 ± 0.090	1.67 ± 0.140	168 ± 3.091	99.88 ± 0.049
17	FBPT17	0.520 ± 0.058	120.38 ± 0.320	3.67 ± 0.149	11.15 ± 0.151	2.12 ± 0.094	156 ± 2.828	97.79 ± 0.268

Values are expressed as mean ± S.D., $n = 3$

The test results in Table 5 are equipped with regression, and the final equation for data analysis to achieve the coding factor is seen in Eq. (7).

$$\begin{aligned} \text{R2 (Steady state flux)} = {} & 390.80 + 24.45{*}\text{A} + 5.15{*}\text{B} \\ & +56.64{*}\text{C-}1.32{*}\text{AB} \\ & +14.56{*}\text{AC} + 1.20 \\ & {*}\text{BC-}15.75{*}\text{A}^2\text{-}11.36{*}\text{B}^2\text{-}6.90{*}\text{C}^2 \end{aligned} \quad (7)$$

The overall p value of the model is 0.0001< 0.05, suggesting that the regression equation is very significant, and the "lack of p value fitting" is 0.5192 > 0.05, implying that the lack of fitting is insignificant. It means that the equation's fitting degree is comparatively fine. In the experimental regression equation, regression study (Table 5) found that the terms A and C had a very important impact on transdermal image flux. There was a significant influence of the permeation enhancer on steady-state flux ($p < 0.05$).

The cumulative amount of drug permeated in 24 h (Q_{24}) response

Response 3: Cumulative amount of drug permeated in 24 h (Q_{24})

The 29.86 Model F value means that the model is significant. p values of less than 0.0500 demonstrate that model terms are significant. A and C are important model terms in this case. Values greater than 0.1000 mean the terms of the model are not significant. In contrast to the pure error, the Lack of Fit F value of 0.5079 means that the Lack of Fit is not significant. There is a

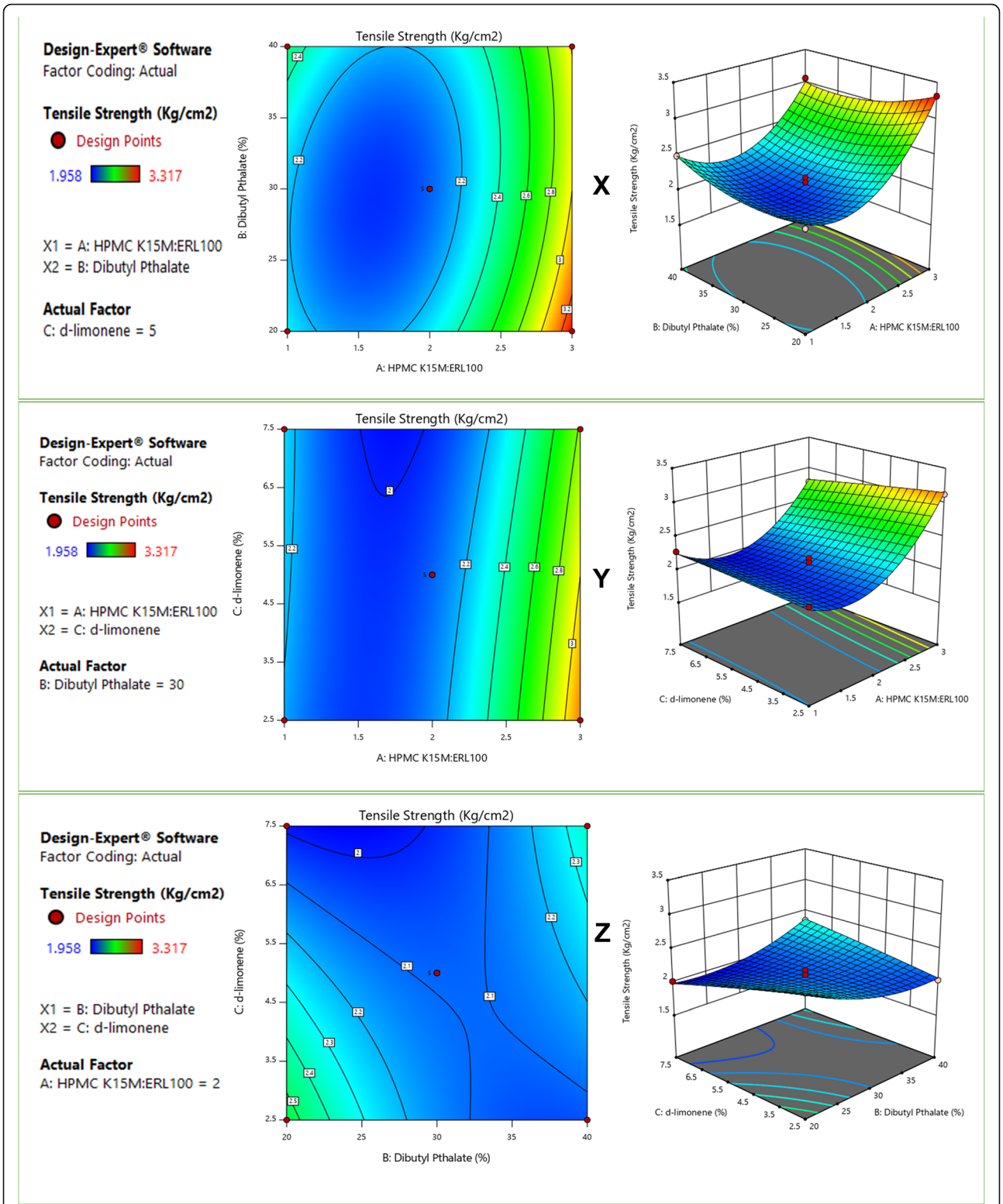

Fig. 3 Response surface plot showing effect of **X** polymer (HPMC K15M:ERL100) ratio (**a**) and di-butyl phthalate (% w/w) (**b**); **Y** polymer (HPMC K15M:ERL100) ratio (**a**) and concentration of d-limonene (% w/w) (**c**); **Z** di-butyl phthalate (% w/w) (**b**) and concentration of d-limonene (% w/w) (**c**) on response R_1 (tensile strength)

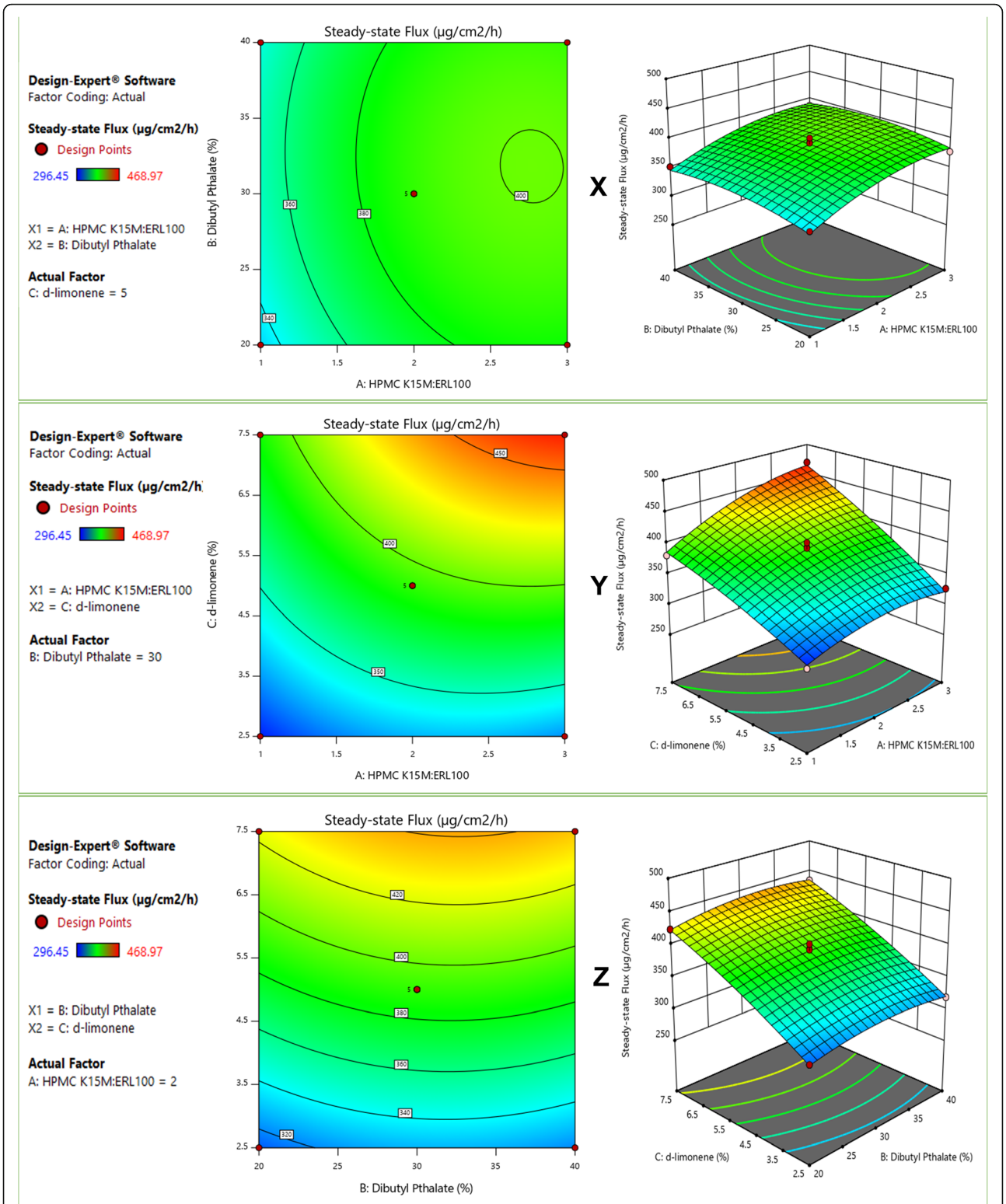

Fig. 4 Response surface plot showing effect of **X** polymer (HPMC K15M:ERL100) ratio (**a**) and di-butyl phthalate (% w/w) (**b**); **Y** polymer (HPMC K15M:ERL100) ratio (**a**) and concentration of d-limonene (% w/w) (**c**); **Z** di-butyl phthalate (% w/w) (**b**) and concentration of d-limonene (% w/w) (**c**) on response R_2 (steady-state flux)

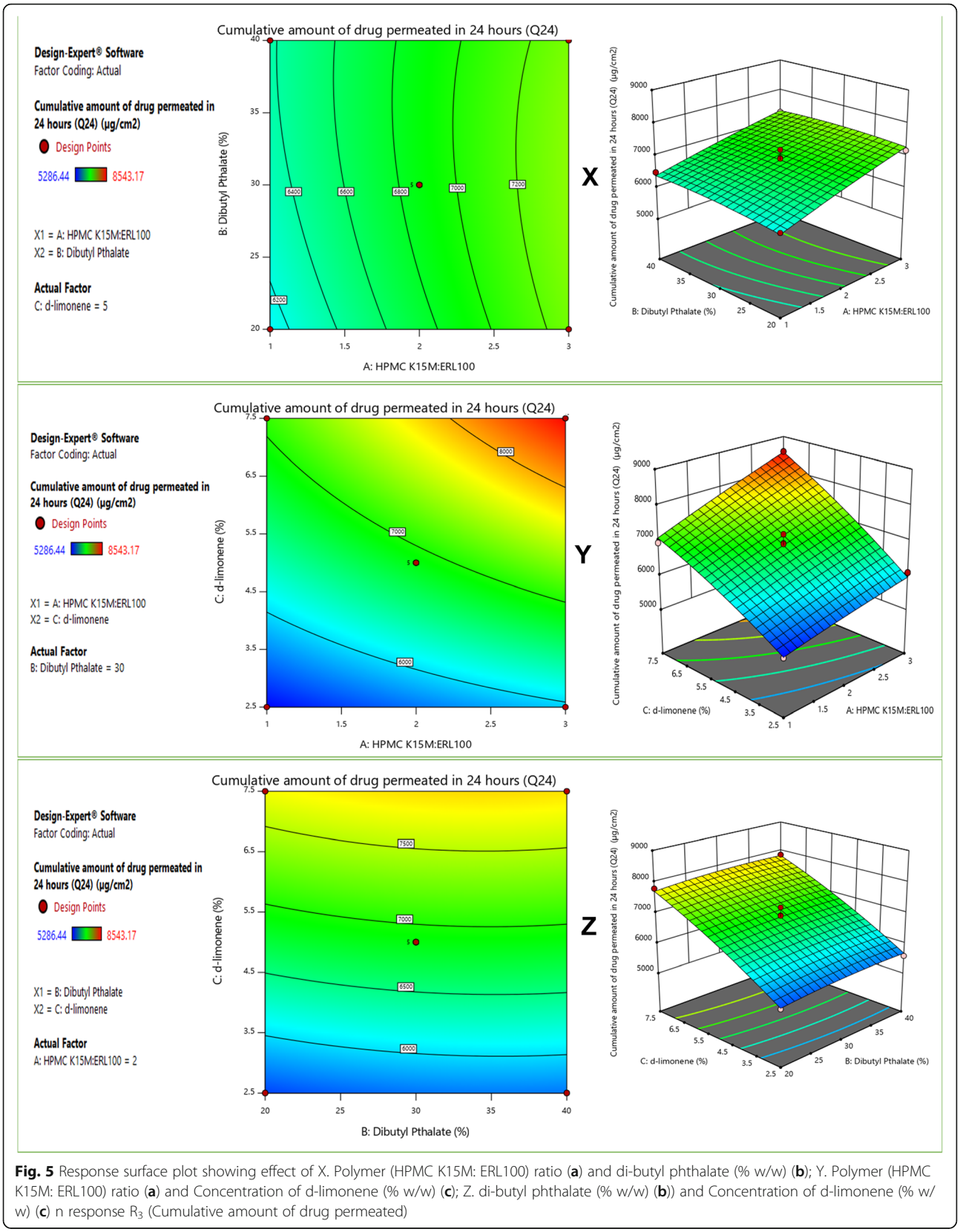

Fig. 5 Response surface plot showing effect of X. Polymer (HPMC K15M: ERL100) ratio (**a**) and di-butyl phthalate (% w/w) (**b**); Y. Polymer (HPMC K15M: ERL100) ratio (**a**) and Concentration of d-limonene (% w/w) (**c**); Z. di-butyl phthalate (% w/w) (**b**)) and Concentration of d-limonene (% w/w) (**c**) n response R_3 (Cumulative amount of drug permeated)

Table 4 ANOVA for the quadratic model (tensile strength response)

Source	Sum of squares	df	Mean square	*F* value	*p* value	
Model	2.82	9	0.3136	53.06	< 0.0001	Significant
A-HPMC K15M:ERL100	1.19	1	1.19	200.75	< 0.0001	
B-Di-butyl pthalate	0.0047	1	0.0047	0.7878	0.4042	
C-d-limonene	0.0343	1	0.0343	5.81	0.0468	
AB	0.0648	1	0.0648	10.96	0.0129	
AC	0.0416	1	0.0416	7.04	0.0328	
BC	0.1875	1	0.1875	31.72	0.0008	
A^2	1.15	1	1.15	194.09	< 0.0001	
B^2	0.1118	1	0.1118	18.92	0.0034	
C^2	0.0005	1	0.0005	0.0906	0.7722	
Residual	0.0414	7	0.0059			
Lack of Fit	0.0135	3	0.0045	0.6468	0.6247	Not significant
Pure error	0.0279	4	0.0070			
Cor total	2.86	16				

69.78% probability that because of noise, a loss of Fit *F* value this high will occur. Non-substantial lack of fit is fine.

The test results in Table 6 are equipped with regression, and the final equation for data analysis to achieve the coding factor is seen in Eq. (8).

$$\begin{aligned} &\text{R3 (Cumulative amount of drug permeated in 24 hours (Q24))} \\ &= 6872.54 + 521.45{*}\text{A} + 71.66{*}\text{B} \\ &+1089.14{*}\text{C-}57.35{*}\text{AB} + 200.11{*}\text{AC-}11.25 \\ &{*}\text{BC-}33.23{*}\text{A}^2\text{-}71.00{*}\text{B}^2\text{-}124.61{*}\text{C}^2 \end{aligned} \quad (8)$$

The overall *p* value of the model is 0.0001 < 0.05, suggesting that the regression equation is very significant, and the "lack of *p* value fitting" is 0.6978 > 0.05, implying that the lack of fitting is insignificant. It means that the equation's fitting amount is comparatively fine.

Regression investigation of the experimental regression equation (Table 6) showed that *A* and *C* terms had a very significant impact on the transdermal film cumulative amount of drug permeated within 24 h (Q_{24}). An important influence of the permeation enhancer on the cumulative amount of drug permeated within 24 h (Q_{24}) was observed ($p < 0.05$).

In vitro drug dissolution study

In vitro dissolution experiments are essential for confirming the performance of sustained release and the reproducibility

Table 5 ANOVA for the quadratic model (steady-state flux response)

Source	Sum of squares	df	Mean square	*F* value	*p* value	
Model	33488.02	9	3720.89	47.54	< 0.0001	Significant
A-HPMC K15M:ERL100	4783.89	1	4783.89	61.12	0.0001	
B-Di-butyl pthalate	211.87	1	211.87	2.71	0.1439	
C-d-limonene	25660.19	1	25660.19	327.86	< 0.0001	
AB	7.02	1	7.02	0.0897	0.7732	
AC	847.68	1	847.68	10.83	0.0133	
BC	5.74	1	5.74	0.0733	0.7944	
A^2	1044.94	1	1044.94	13.35	0.0081	
B^2	543.70	1	543.70	6.95	0.0336	
C^2	200.23	1	200.23	2.56	0.1537	
Residual	547.86	7	78.27			
Lack of Fit	219.20	3	73.07	0.8893	0.5192	Not significant
Pure error	328.66	4	82.16			
Cor Total	34035.88	16				

Table 6 ANOVA for the quadratic model {cumulative amount of drug permeated in 24 h (Q_{24}) response}

Source	Sum of squares	df	Mean square	*F* value	*p* value	
Model	1.198E+07	9	1.331E+06	29.86	< 0.0001	Significant
A-HPMC K15M:ERL100	2.175E+06	1	2.175E+06	48.80	0.0002	
B-Di-butyl pthalate	41075.66	1	41075.66	0.9214	0.3691	
C-d-limonene	9.490E+06	1	9.490E+06	212.88	< 0.0001	
AB	13157.35	1	13157.35	0.2952	0.6038	
AC	1.602E+05	1	1.602E+05	3.59	0.0999	
BC	506.30	1	506.30	0.0114	0.9181	
A^2	4649.90	1	4649.90	0.1043	0.7562	
B^2	21226.92	1	21226.92	0.4762	0.5124	
C^2	65378.56	1	65378.56	1.47	0.2652	
Residual	3.120E+05	7	44577.82			
Lack of Fit	86074.35	3	28691.45	0.5079	0.6978	Not significant
Pure error	2.260E+05	4	56492.60			
Cor total	1.229E+07	16				

of the rate and period of release of the drug. Dissolution tests for various preparations were carried out via phosphate buffer, pH 7.4, as dissolution media at 32 °C, in a USP Dissolution Apparatus V paddle over the disc. The release study of transdermal films (FBPT1 to FBPT9) and (FBPT10 to FBPT17) containing different ratios of HPMC K15M and ERL100 are shown in Figs. 6 and 7. It was found that as the concentration of HPMC K15M (hydrophilic polymer) increased in the formulations, the dissolution rate was increased successively. Transdermal film FBPT7 has the highest drug release 97.749 ± 2.928% at the end of 24 h while FBPT5 has a minimum drug release 80.496 ± 4.347% amongst all 17 formulations. It was found that the release of FBP reduced as the proportion of HPMC K15M declined and the proportion of ERL100 was amplified. This is because of the hydrophilic nature of HPMC K15M and hydrophobic nature of the ERL100 polymer.

Another parameter also associated with drug release profile is the concentration of penetration enhancer, i.e. d-limonene, used. It played a role in the release profile of FBP via as concentration increased the release of FBP increased. D-limonene, a cyclic terpene that is free of harmful special effects, has been used in the transdermal delivery of many drugs as a penetration enhancer [28].

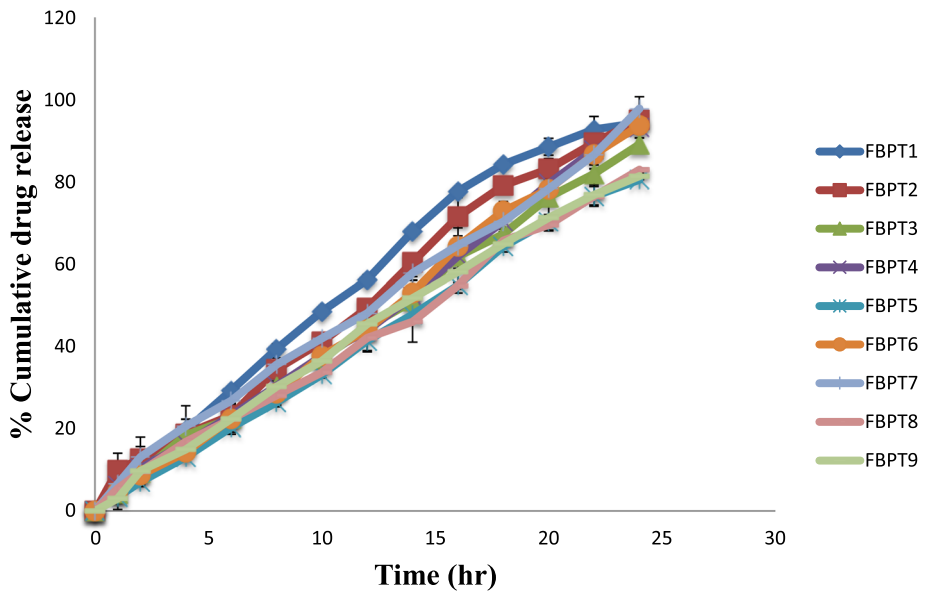

Fig. 6 In vitro drug release profile of transdermal films (FBPT1-FBPT9)

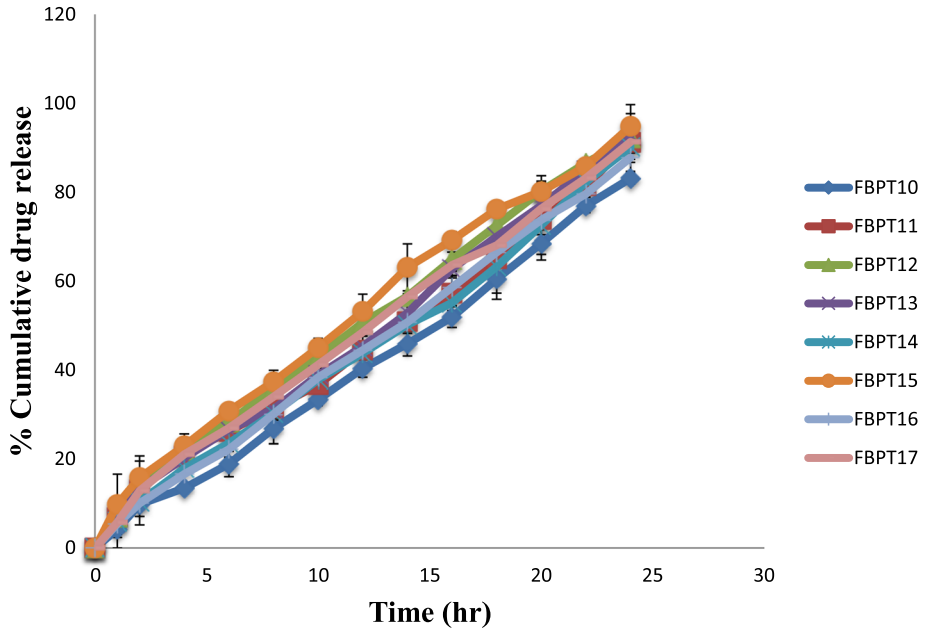

Fig. 7 In vitro drug release profile of transdermal films (FBPT10-FBPT17)

Model fitting

To illustrate the release kinetics of FBP from the transdermal film, in vitro drug release was fitted into various equations and kinetic models. The zero-order equation, first-order equation, Higuchi kinetics model, Hixon–Crowel kinetics model and Korsmeyer–Peppas models were the kinetic models used (Table 7). As demonstrated by the uppermost correlation coefficients (R^2 = 0.982–0.999), all the formulations adopted zero-order release. A non-Fickian transport function was suggested by the n value ($0.87 > n > 0.5$) derived from the log mt/mT vs log time curve (Korsmeyer–Peppas) slope.

Table 7 Model fitting kinetics for in vitro release profile from different transdermal films

Formulation code	Zero-order kinetics (R^2)	First-order kinetics (R^2)	Higuchi kinetics model (R^2)	Hixon–Crowel kinetics model (R^2)	Korsmeyer–Peppas kinetics	
					R^2	n
FBPT1	0.982	0.953	0.979	0.985	0.994	0.603
FBPT2	0.992	0.902	0.955	0.960	0.967	0.533
FBPT3	0.998	0.920	0.963	0.964	0.996	0.755
FBPT4	0.996	0.876	0.948	0.940	0.990	0.649
FBPT5	0.998	0.959	0.964	0.981	0.999	0.870
FBPT6	0.997	0.881	0.954	0.948	0.995	0.759
FBPT7	0.997	0.750	0.964	0.894	0.995	0.598
FBPT8	0.996	0.939	0.956	0.969	0.955	0.667
FBPT9	0.996	0.972	0.979	0.991	0.988	0.865
FBPT10	0.996	0.924	0.949	0.966	0.990	0.744
FBPT11	0.994	0.863	0.949	0.931	0.990	0.565
FBPT12	0.998	0.914	0.975	0.966	0.996	0.573
FBPT13	0.997	0.872	0.953	0.940	0.988	0.553
FBPT14	0.995	0.872	0.951	0.935	0.995	0.638
FBPT15	0.995	0.889	0.978	0.961	0.993	0.490
FBPT16	0.999	0.924	0.964	0.967	0.996	0.673
FBPT17	0.998	0.905	0.975	0.962	0.995	0.622

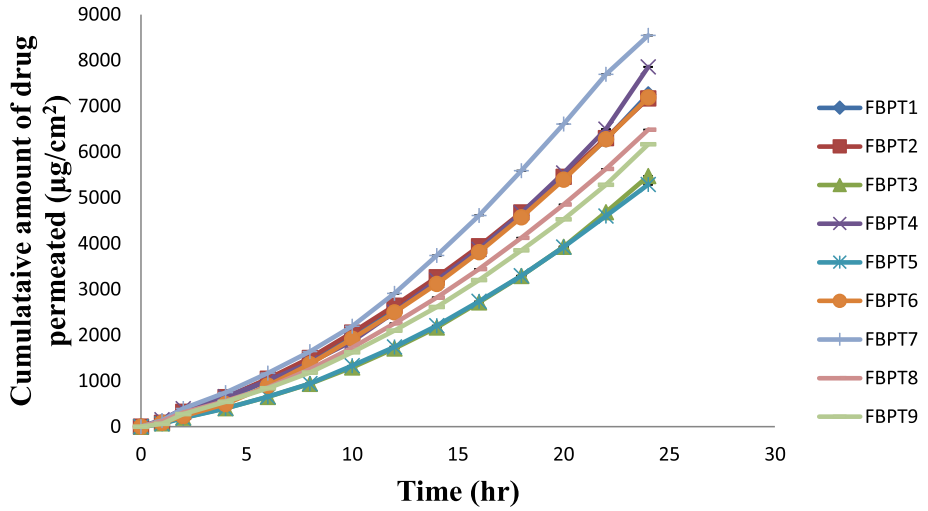

Fig. 8 Ex vivo drug permeation profile of flurbiprofen from transdermal films (FBPT1-FBPT9)

Ex vivo drug permeation study

D-limonene had a possible enhancement effect on FBP permeation through the porcine skin in our initial research. The ex vivo permeation of FBP concluded via porcine skin is revealed in Figs. 8 and 9, and permeation parameters, Q_{24}, flux and permeability coefficient in Table 2. The Q_{24} ranged from 5286.44 ± 8.539 to 8543.17 ± 1.939 µg/cm^2, while flux ranged from 296.45 ± 6.412 to 468.97 ± 8.294 µg/cm^2/h and permeability coefficient ranged from $0.988\times10^{-2}\pm0.075$ to $1.563\times10^{-2}\pm0.065$. Formulation FBPT7 showed the highest amount of FBP permeated (8543.17 ± 1.939 µg/cm^2) with a flux of 468.97 ± 8.294 µg/cm^2/h. The enhancement ratio of FBPT7 compared with the transdermal film of FBP without penetration enhancer was 4.41 fold higher. The d-limonene permeation enhancement effect indicates that several pathways are probable that may have resulted in a more permeable intercellular pathway for FBP. These involve the partitioning of FBP into lipids of the stratum corneum (SC), the partial extraction of SC lipids [29] and the phase separation inside the SC lipid lamellae. The FBPT7 formulation demonstrated the highest Q_{24} and flux between the preparations and was statistically significant ($p < 0.05$) as well.

Skin irritation test

The skin irritation investigation aims to make sure the irritation behaviour of the FBP transdermal film for the score of skin irritation (erythema and oedema). In Table 8, the

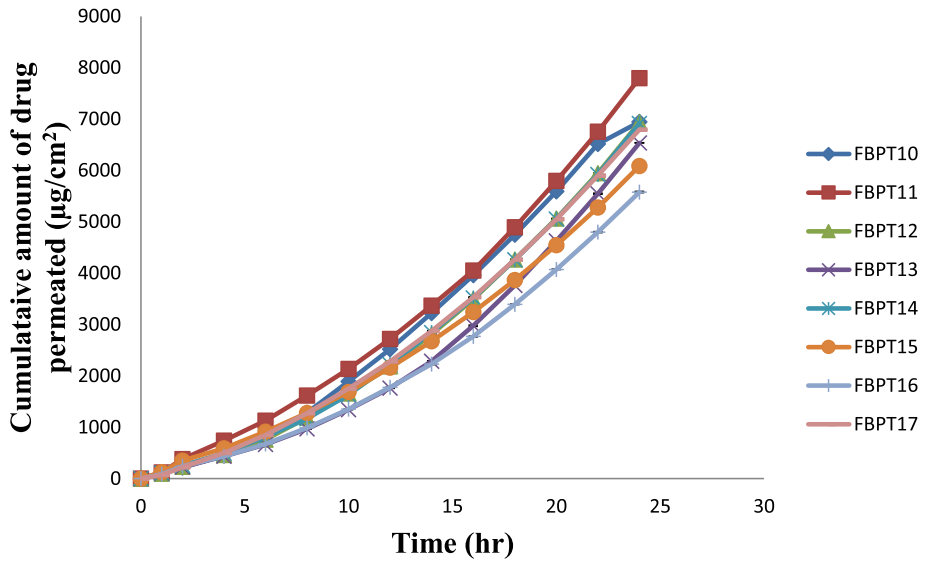

Fig. 9 Ex vivo drug permeation profile of flurbiprofen from transdermal films (FBPT10-FBPT17)

Table 8 Skin irritation studies on Wistar male rat

Group	Visual observation	
	Erythema	Oedema
Negative control	0.00 ± 0.000	0.00 ± 0.000
Adhesive tape	0.91 ± 0.023	0.58 ± 0.016
FBPT7 transdermal film	0.16 ± 0.065	0.41 ± 0.047
Formalin	3.33 ± 0.084	3.25 ± 0.72

Values are expressed as mean ± S.D., $n = 3$

results for that are shown. Compounds producing scores of 2 or less are considered negative (no skin irritation), according to the Draize scoring criteria. The transdermal formulations produced are, therefore, free from skin irritation [30].

Discussion

Matrix-type transdermal film of FBP was prepared with d-limonene as a penetration enhancer and DBP as a plasticizer by different ratios with various hydrophilic and hydrophobic polymers like HPMC K15M and ERL100 which were found to be transparent, smooth and wrinkle-free. By this approach, all cautions related to FBP conventional dosage form were diminished with maximum efficacy of the drug for effective management of RA [31]. The FT-IR spectra of the pure FBP, HPMC K15M, ERL100 and their physical mixture are presented in Fig. 1. In all the samples, the main peaks of the drug detected indicate no chemical interface between the drug and the polymers. In matrix-type films, the polymers cast-off are frequently used and are compatible with a numeral of drugs [32]. At 118.03 °C, the thermogram obtained for pure FBP exerted a steep endothermic peak that correlated with the melting temperature of the FBP (Fig. 2). In the case of a physical combination, the characteristic peak of the substance was also detected. To determine the physicochemical consistency of the formulation, the prepared films were assessed for their physicochemical parameters. In vitro release tests have been exposed to films of appropriate qualities. The release investigation is important because, to ensure a steady drug permeation rate, the drug concentration on the surface of the stratum corneum must be maintained continuously and retained considerably higher than the drug concentration in the body. To illustrate the release kinetics of FBP from transdermal films, in vitro release data from formulations of each batch was fitted to various equations and kinetic models. All formulations were accompanied by the zero-order release. For the zero-order model, the value of the correlation coefficient was greater than in other models. It was therefore clear that the formulation adopted the kinetic zero order [33]. In the present study, polymer (HPMC K15:ERL100) ratio as film-forming polymers, the concentration of di-butyl phthalate (% w/w) as plasticizer and the concentration of d-limonene (% w/w) as penetration enhancer are defined as independent variables, and tensile strength (kg/cm^2), steady-state flux (μg/cm^2/h) and the cumulative amount of drug permeated in 24 h (Q_{24}) (μg/cm^2) are considered as dependent variables. In the next step, the Box–Behnken response surface design was chosen, followed by the implementation of 17 experiments with 5 central points. The sequential model sum of the square test for tensile strength response reveals that quadratic models were important as their consistent p values were respectively $0.0001 < 0.05$. Quadratic models were found to be important at p values of $0.0001 < 0.05$, respectively, in the case of steady-state flux response. Quadratic models were found to be important at p values $0.0001 < 0.05$, respectively, for the cumulative amount of drug permeated in 24 h (Q_{24}) [34].

Polymer (HPMC K15M:ERL100) ratio 3:1, 30% dibutyl phthalate concentration and 7.5% d-limonene concentration are the optimal conditions for developing transdermal film of FBP predicted in the interest ramp for optimization. Under the above conditions, 2.783 ± 0.312 kg/cm^2, 468.97 ± 8.294 μg/cm^2/h and 8543.17 ± 1.939 μg/cm^2 were observed as the predicted tensile strength, steady-state flux and cumulative amount of drug permeated within 24 h (Q_{24}). Chemical penetration enhancers which are typically potent irritants to the skin and concentrations necessary for attaining suitable penetration levels produce hyperkeratosis, marked acanthosis and stratum corneum with ulcerative eruptions. All these associated problems can be resolved to a large extent by the use of natural moieties as penetration enhancers. Via one or more of the mechanisms interacting with SC lipids and/or keratin, terpenes can increase skin permeability and increase drug solubility into SC lipids [5]. Some lipophilic drugs such as ketoprofen and valsartan [35, 36] have also been found to be compatible with hydrocarbon d-limonene. The great enhancement of limonene shows that there could have been some pathways that may have contributed to a more permeable FBP pathway. Increased solubility of FBP within the skin, partial stratum corneum (SC) lipid extraction [29] and phase separation within SC lipid lamellae [37] were included.

Conclusions

The current research determines that the FBP transdermal film can be produced and optimized using different concentrations of polymeric excipients (HPMC K15M to ERL100 ratio), a plasticizer (di-butyl phthalate) and penetration enhancer (d-limonene) by Box–Behnken statistical design. Based on the outcomes of this research, it can be concluded that the film FBPT7 was able to accomplish a well-controlled release and effective skin

penetration of the drug in the incidence of permeation enhancers for long periods. The preparation constituents have a direct effect on the product performance; polymer matrix enhances the elasticity and sustained drug release, and the plasticizer enhances the tensile strength and the permeation enhancer increases the drug flux. The polymer blend of HPMC K15M/ERL100 may have the ability to formulate a transdermal drug delivery system because they have good mechanical strength and film formation property. The developed TDDS of FBP may prove a better alternative to a conventional dosage form in the effective management of RA for the long term.

However, more in vivo pharmacokinetic experiments may be carried out to demonstrate the relevance of the effects of in vivo pharmacodynamic studies of in vitro penetration and to assess the therapeutic level of the drug.

Abbreviations

ANOVA: Analysis of variance; COX: Cyclooxygenase enzyme; CPCSEA: Committee for purpose of control and supervision of experiments on animals; DBT: Di-butyl phthalate; DSC: Differential scanning calorimetry; ERL100: Eudragit RL100; FBP: Flurbiprofen; FT-IR: Fourier transform infrared spectroscopy; FBPT: Flurbiprofen transdermal drug delivery system; HPMC K15M: Hydroxy propyl methyl cellulose; NSAIDs: Non-steroidal anti-inflammatory drugs; PGG2: Prostaglandin G2; PGH2: Prostaglandin H2; PBS: Phosphate-buffered saline; Q_{24}: Cumulative amount of drug permeated in 24 h; RA: Rheumatoid arthritis; SC: Stratum corneum; RH: Relative humidity; USP: United State pharmacopoeia

Acknowledgements

The authors express special thanks to Dr. Suman Jain, Director School of Studies in Pharmaceutical Sciences, Jiwaji University, Gwalior (M.P), and Dr. Mukul Tailang, Professor School of Studies in Pharmaceutical Sciences, Jiwaji University, Gwalior (M.P), for their valuable guidance and kind support.

Authors' contributions

'RJ' designed and optimizes the study and developed the methodology. 'RJ' performed the experiments, collection and interpretation of data. 'RJ' wrote the manuscript. 'NG' contributed to manuscript revision and provided supervision. 'RJ' and 'NG' read and approved the final manuscript.

Funding

This research did not receive any specific grant from funding agencies in the public, commercial or not-for-profit sectors.

Availability of data and materials

The datasets of research were collected from experiments and analysis of variables during the current study. These datasets are available from the corresponding author on reasonable request.

Ethics approval and consent to participate

The ex vivo drug permeation study work was completed at Jiwaji University, Gwalior, according to the protocols permitted by the Committee for Purpose of Control and Supervision of Experiments on Animals (CPCSEA), Ministry of Social Justice and Empowerment, Government of India, under the reference no. IAEC/JU/50 on the recommendations of the Institutional Animal Ethical Committee of Jiwaji University (Gwalior, India).

Consent for publication

Not applicable.

Competing interests

The authors declare no competing interests.

Received: 9 November 2020 Accepted: 4 February 2021
Published online: 03 March 2021

References

1. Breimer DD (1984) Rationale for rate-controlled drug delivery of cardiovascular drugs by the transdermal route. Ame Heart J 108(1):196–200
2. Akram W, Joshi R, Garud N (2019) Inulin: a promising carrier for controlled and targeted drug delivery system. J Drug Del Ther 9(1-s):437–441
3. Naik A, Kalia YN, Guy RH (2000) Transdermal drug delivery: overcoming the skin's barrier function. Pharm Sci Tech Today 9:318–326
4. Cornwell PA, Barry BW, Bouwstra JA, Gooris GS (1996) Modes of action of terpene penetration enhancers in human skin; differential scanning calorimetry, small-angle X-ray diffraction and enhancer uptake studies. Int J Pharm 127(1):9–26
5. Williams AC, Barry BW (1991) Terpenes and the lipid–protein–partitioning theory of skin penetration enhancement. Pharm Res 8(1):17–24
6. Okabe H, Suzuki E, Saitoh T, Takayama K, Nagai T (1994) Development of novel transdermal system containing d-limonene and ethanol as absorption enhancers. J cont rel 32(3):243–247
7. Aletaha D, Neogi T, Silman AJ, Funovits J, Felson DT, Bingham CO III, Birnbaum NS, Burmester GR, Bykerk VP, Cohen MD, Combe B (2010) Rheumatoid arthritis classification criteria: an American College of Rheumatology/European League Against Rheumatism collaborative initiative. Arthritis Rheum 62(9):2569–2581
8. Symmons DP (2002) Epidemiology of rheumatoid arthritis: determinants of onset, persistence and outcome. Bes Prac Res Clin Rheu 16(5):707–722
9. Thakur S, Riyaz B, Patil A, Kaur A, Kapoor B, Mishra V (2018) Novel drug delivery systems for NSAIDs in management of rheumatoid arthritis: an overview. Biomed Pharmacother 106:1011–1023
10. Brogden RN, Heel RC, Speight TM, Avery GS (1979) Flurbiprofen: a review of its pharmacological properties and therapeutic use in rheumatic diseases. Drugs 18(6):417–438
11. Teixeira AV, Pocas L, Serrao D (1984) Study of the gastric mucosa in rheumatic patients before and after the administration of flurbiprofen. Brit J Clinic Praesit 32:222–227
12. Akram W, Garud N (2020) Optimization of inulin production process parameters using response surface methodology. Future J Pharm Sci 6(1):1–9
13. Box GE, Behnken DW (1960) Some new three level designs for the study of quantitative variables. Technometrics 2(4):455–475
14. Saoji SD, Atram SC, Dhore PW, Deole PS, Raut NA, Dave VS (2015) Influence of the component excipients on the quality and functionality of a transdermal film formulation. Aaps Pharmscitech 16(6):1344–1356
15. Joshi R, Raje S, Akram W, Garud N (2019) Particle engineering of fenofibrate for advanced drug delivery system. Future J Pharm Sci 5(1):14
16. JOSHI R, AKRAM W, Garud N, Dubey A, Bhadkariya S (2018) Development and optimization of orodispersible tablets using solid dispersion of Telmisartan. J Drug Del and Ther 8(6):171–178
17. David SR, Rajabalaya R, Zhia ES (2015) Development and in vitro evaluation of self-adhesive matrix-type transdermal delivery system of ondansetron hydrochloride. Trop J Pharm Res 14(2):211–218
18. Akhlaq M, Arshad MS, Mudassir AM, Hussain A, Kucuk I, Haj-Ahmad R, Rasekh M, Ahmad Z (2016) Formulation and evaluation of anti-rheumatic dexibuprofen transdermal patches: a quality-by-design approach. J Drug Tar 24(7):603–612
19. Sarkar G, Saha NR, Roy I, Bhattacharyya A, Bose M, Mishra R, Rana D, Bhattacharjee D, Chattopadhyay D (2014) Taro corms mucilage/HPMC based transdermal patch: an efficient device for delivery of diltiazem hydrochloride. Int J Bio Macro 66:158–165
20. Patel DP, Setty CM, Mistry GN, Patel SL, Patel TJ, Mistry PC, Rana AK, Patel PK, Mishra RS (2009) Development and evaluation of ethyl cellulose-based transdermal films of furosemide for improved in vitro skin permeation. Aaps Pharmscitech 10(2):437–442
21. Mamatha T, Rao JV, Mukkanti K, Ramesh G (2010) Development of matrix type transdermal patches of lercanidipine hydrochloride: physicochemical and in-vitro characterization. DARU: Journal of Faculty of Pharmacy, Tehran University of Medical Sciences 18(1):9.
22. Kusum Devi V, Saisivam S, Maria GR, Deepti PU (2003) Design and evaluation of matrix diffusion controlled transdermal patches of verapamil hydrochloride. Drug Dev Ind Pharm 29(5):495–503
23. Aggarwal G, Dhawan S, Hari Kumar SL (2013) Formulation, in vitro and in vivo evaluation of transdermal patches containing risperidone. Drug Dev Indu Pharm 39(1):39–50

24. Parhi R, Suresh P (2016) Transdermal delivery of Diltiazem HCl from matrix film: effect of penetration enhancers and study of antihypertensive activity in rabbit model. J Adv Res 7(3):539–550
25. Ammar HO, Ghorab M, Mahmoud AA, Makram TS, Ghoneim AM (2013) Rapid pain relief using transdermal film forming polymeric solution of ketorolac. Pharm Dev Tech 18(5):1005–1016
26. Sundralingam U, Muniyandy S, Radhakrishnan AK, Palanisamy UD (2020) Ratite oils for local transdermal therapy of 4-OH tamoxifen: development, characterization, and ex vivo evaluation. J Lip Res 28:1–3
27. Ubaidulla U, Reddy MV, Ruckmani K, Ahmad FJ, Khar RK (2007) Transdermal therapeutic system of carvedilol: effect of hydrophilic and hydrophobic matrix on in vitro and in vivo characteristics. Aaps Pharmscitech 8(1):E13–E20
28. Tipre DN, Vavia PR (2003) Acrylate-based transdermal therapeutic system of nitrendipine. Drug Dev Indus Pharm 29(1):71–78
29. Krishnaiah YS, Satyanarayana V, Bhaskar P (2002) Effect of limonene on the in vitro permeation of nicardipine hydrochloride across the excised rat abdominal skin. Die Pharmazie 57(12):842–847
30. Draize JH (1944) Methods for the study of irritation and toxicity of substances applied topically to the skin and mucous membranes. J Pharmacol Exp Ther 82: 377–390
31. Vijaya R, Ruckmani K (2011) In vitro and in vivo characterization of the transdermal delivery of sertraline hydrochloride Films. DARU J Pharm Sci 19(6):424
32. Agrawal MB, Patel MM (2020) Optimization and in vivo evaluation of quetiapine-loaded transdermal drug delivery system for the treatment of schizophrenia. Drug Dev Indus Pharm 16:1–3
33. Sharma P, Tailang M (2020) Design, optimization, and evaluation of hydrogel of primaquine loaded nanoemulsion for malaria therapy. Future J Pharm Sci 6(1):1–1
34. Gannu R, Yamsani VV, Yamsani SK, Palem CR, Yamsani MR (2009) Optimization of hydrogels for transdermal delivery of lisinopril by Box–Behnken statistical design. Aaps Pharmscitech 10(2):505–514
35. Rhee YS, Choi JG, Park ES, Chi SC (2001) Transdermal delivery of ketoprofen using microemulsions. Int J Pharm 228(1-2):161–170
36. Rizwan M, Aqil M, Ahad A, Sultana Y, Ali MM (2008) Transdermal delivery of valsartan: I. Effect of various terpenes. Drug Dev Indus Pharm 34(6):618–626
37. Moghimi HR, Williams AC, Barry BW (1997) A lamellar matrix model for stratum corneum intercellular lipids. V. Effects of terpene penetration enhancers on the structure and thermal behaviour of the matrix. Int J Pharm 146(1):41–54

Publisher's Note

Springer Nature remains neutral with regard to jurisdictional claims in published maps and institutional affiliations.

Submit your manuscript to a SpringerOpen journal and benefit from:

► Convenient online submission
► Rigorous peer review
► Open access: articles freely available online
► High visibility within the field
► Retaining the copyright to your article

Submit your next manuscript at ► springeropen.com